Corrosion and Degradation in MEA based post-combustion CO_2 Capture

Georgios Fytianos[a], Seniz Ucar[a], Andreas Grimstvedt[b], Astrid Hyldbakk[b], Hallvard F. Svendsen[a], Hanna K. Knuutila[a]*

[a]Norwegian University of Science and Technology,7491 Trondheim, Norway
[b]SINTEF Materials and Chemistry, 7465 Trondheim, Norway

Abstract

Two of the main challenges in post-combustion CO_2 capture with ethanolamine are solvent degradation and material corrosion. It has been shown that there is a correlation between degradation and corrosion. The present paper examines this correlation by studying the effect of 10 MEA degradation products on corrosion. Thermal degradation experiments were conducted under stripper conditions for 5 weeks. 30wt% MEA solution with 1wt% of the various degradation products were placed in 316 SS cylinders and stored in a thermostat chamber at 135 °C. ICP-MS was used for the metal concentration analyses for all the solutions, while ion chromatography was used for the quantitative determination of heat stable salts anions and MEA concentrations. The solutions were also analyzed for degradation products in order to study the formation and thermal stability of these compounds. For corrosion monitoring, in addition to ICP-MS analyses, SEM-EDS was used for examining the cylinders surface morphology and elemental composition while XRD was used for corrosion product identification. In the present paper, the influence of the secondary degradation products on corrosion is studied. Results show that some specific degradation products, like bicine, HeGly and HEEDA enhance corrosion while others don't seem to have a significant effect on corrosion of stainless steel.

Keywords: Corrosion; MEA; CO_2 capture; degradation

**Corresponding author. Tel.: +47 73594119; fax: +47 735 94080.*
E-mail address: hanna.knuutila@ntnu.no

1. Introduction

It is crucial to develop robust and environmentally benign technologies for CO_2 emissions reduction. In this direction, CO_2 capture and storage is one potent strategy to minimize the emissions of carbon dioxide from fossil fuel power plants. An effective CO_2 capture method is to remove CO_2 after combustion (post-combustion CO_2 capture) by chemical absorption using various aqueous amine solutions. Today, this is the most mature method for post-combustion CO_2 capture and has already reached commercial stage[1]. Absorption using amines as solvents has been applied successfully for several decades in areas such as natural gas processing or coal gasification[2], but also in smaller for post combustion capture e.g. AES Corporation CO_2 plant in Warrior Run, Maryland[3]. Various alkanoamines can be used for CO_2 post-combustion capture. Monoethanolamine (MEA) is nowadays the benchmark solvent, due to its good properties towards CO_2 (fast absorption rate, cheap and reasonable volatility)[4].

Solvent degradation and equipment corrosion are two of the main problems in CO_2 capture processes. By definition, degradation is the irreversible transformation of an absorbent solution into other compounds. These byproducts can cause problems to the system such as corrosion of the equipment, amine loss, fouling, foaming and reduction of CO_2 absorption capacity[5].

Experience shows that amine degradation products often aggravate corrosion[5], and corrosion and degradation are closely tied since the byproducts of ethanolamine (MEA) have been shown to increase corrosion rates[6, 7]. Degradation of amines can be oxidative or thermal, and as mentioned above, some of the degradation products are corrosive agents. Oxidative degradation due to dissolved O_2 is found to be more dominant than thermal degradation in pilot plants[8-10], and has been studied by various researchers [11-13]. This is likely also the case in industrial plants. A detailed overview of MEA oxidative degradation and the degradation compounds' mechanisms can be found elsewhere [8]. The primary oxidative degradation compounds are ammonia, aldehydes and carboxylic acids. Anions of strong carboxylic acids, e.g. formic acid and oxalic acid, form with MEA the so called heat-stable salts (HSS). HSS reduce the CO_2 capture capacity, and induce corrosion in gas treating power plants. The role of formation of heat stable salts (HSS) on corrosion has also been studied in [14-16]. Among HSS formate and oxalate have a higher impact on corrosion than the rest HSS. The effect of five carboxylic acids(oxalic, acetic, glycolic, propionic and formic) on corrosion have been studied previously by Fytianos et al.[16]. 30wt% MEA solution containing 1wt% oxalic acid and 30wt% MEA solution with 1wt% formic acid showed higher impact on corrosion compared to the other tested acids.

Also thermal degradation of MEA has been studied by various researchers [9, 17, 18] and their findings are in good agreement with regard to degradation products formation mechanisms. The secondary degradation compounds are defined as products formed by reaction of MEA with the primary degradation compounds[8]. The three main thermal degradation products are HEIA, HEEDA and OZD with HEIA being the dominant one. Degradation rates increase with temperature and CO_2 loading.

There are various factors that can enhance the corrosiveness in MEA based CO_2 capture. Operating parameters (such as amine concentration, process temperature, CO_2 and O_2 content, HSS and impurities) determine the extent of corrosion within CO_2 capture plants[19, 20]. Generally, an increase in amine concentration, CO_2 loading, temperature and O_2 will increase the corrosion rate of carbon steel in MEA based pilot plant[21].

Lately, stainless steel has become more popular in coal fired post-combustion CO_2 capture (PCCC) as the major material of the plant [22] . From the review of J. Kittel and S. Gonzalez [23], it is stated that carbon steel should not be the material of choice for PCCC, and that stainless steel 316L has much higher corrosion resistance. The knowledge of corrosion caused by degradation products is limited in the case of stainless steel, which has been reported to suffer aggressive corrosion in the presence of formic acid in MEA plant[24]. According to Davis, stainless steels do not catalyze the thermal degradation of MEA[17].

There is a lack of data with regard to the effect of MEA degradation products on corrosion. The present paper focuses on the effect of 7 oxidative and 3 thermal degradation products on corrosion. The secondary oxidative degradation products of MEA, i.e. HEF, HEA, HEI, HeGly, BHEOX, Bicine and HEPO are tested. In addition, the thermal degradation products HEIA, OZD and HEEDA are tested in this work. In this paper the experimental results from the thermal degradation and corrosion experiments are described and discussed. In addition, the thermal stability and the thermal decomposition of the degradation products are examined. The ultimate goal of this paper is to investigate which of the degradation products of MEA could contribute to high corrosion in the CO_2 capture process.

2. Material and Methods

The chemicals used in this work were MEA, HEEDA, OZD, HEI, Bicine, HEA (Sigma-Aldrich, purity >97%), BHEOX, HEF, HEIA (Alfa Aesar, purity > 97%), HEPO (Tiger Scientific, purity >98%) and HeGly (Enamine, purity >98%). The CAS numbers, full names and structures of the tested degradation products are listed in Table 1.

Table 1:Tested MEA degradation products

Abbreviation	Compound	CAS	Structure
BHEOX	N,N′-Bis(2-hydroxyethyl)-oxamide	1871-89-2	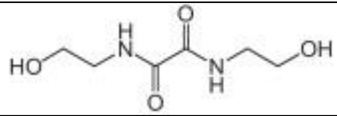
HEA	N-(2-hydroxyethyl)-acetamide	142-26-7	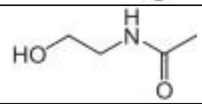
HEF	N-(2-hydroxyethyl)-formamide	693-06-1	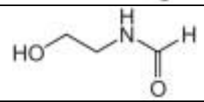
HEGly	N-(2-hydroxyethyl)-glycine	5835-28-9	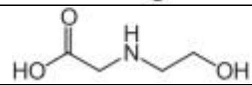
HEI	N-(2-hydroxyethyl)-imidazole	1615-14-1	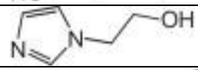
HEPO	4-(2-hydroxyethyl)-2-piperazinone	23936-04-1	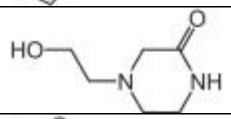
OZD	2-Oxazolidinone	497-25-6	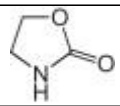
HEIA	N-(2-hydroxyethyl) imidazolidinone	3699-54-5	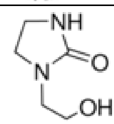
HEEDA	N-(2-hydroxyethyl) ethylenediamine	111-41-1	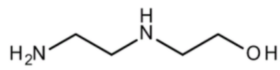
Bicine	N,N-Bis(2-hydroxyethyl)glycine	150-25-4	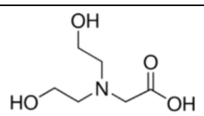

Solutions of 30wt% MEA containing 1wt% of degradation product were prepared gravimetrically with distilled water. The solutions were loaded with CO_2 (0.4 mol CO_2/ mol MEA). 9g of each solution was put into a 316 stainless steel cylinder equipped with Swagelok® end caps. The cylinders were heated in a thermostat chamber at 135 °C for 5 weeks. For each solution, 10 cylinders were used (two parallels for each week). Every week, the two replicates of each solution were tested for total metal concentration and for degradation product formation. A similar approach was previously used by Fytianos et al.[16]. The cylinders were weighed at the start and end of the experiments for possible leakage detection. Corrosion evaluation of the liquid samples was conducted by measuring the metals concentration with ICP-MS and IC was used for the HSS anion analyses. The surface morphology of the inner part of the cylinder was examined with SEM-EDS. After the experiments, XRD was used for the identification of corrosion products. The MEA concentrations after every week were determined with IC and degradation compounds were analysed with LC-MS after week 2 and week 5. A more detailed description of the analytical methods used is given below.

Solutions were analysed for total Fe, Cr, Ni and Mo by a high resolution Thermo Fischer Element 2 ICP-MS, as an indication of corrosivity. Grimstvedt et al. [25] has previously used a similar approach. The approach is based on the fact that higher metal concentrations indicate more corrosion. The initial CO_2 loaded 30wt% MEA solution and the solutions after 5 weeks were analysed for amine concentration and CO_2 content. Total alkalinity of the various solutions was determined by H_2SO_4 titration and the $BaCl_2$ method, see Ma'mun et al. [26], was used for the determination of CO_2 concentrations for the start and end samples.

The quantification of the degradation products was performed using an Agilent 1290 Infinity LC system coupled to an Agilent 6490 Triple Quadrupole Mass Spectrometer equipped with an Agilent Jet Stream ion source (Agilent Technologies, Santa Clara, CA, USA). The components were separated by optimized reverse phase chromatographic methods, using various columns and mobile phases. Retention times were within the range of 1 to 10 minutes, and the limits of quantitation (LOQ) were between 0.1 and 10 ng/ml. Details of the LC-MS methods are listed in Table 2.

Table 2. Overview of the analytical methods used to separate and quantify the degradation products

Analyte	**Column**	**Mobile phase**	**LOQ (ng/ml)**
HEHEAA	Supelco Discovery® HS F5 (3 µm particle size, 15 cm × 4.6 mm)	25 mM Formic acid	0.1
HEEDA	Ascentis® Express RP-Amide, 2.7 micron (2.7 µm particle size, 15 cm × 4.6 mm)	25 mM Formic acid	0.1
Bicine	Supelco Discovery® HS F5 (3 µm particle size, 15 cm × 4.6 mm)	25 mM Formic acid/methanol	1
HeGly	Supelco Discovery® HS F5 (3 µm particle size, 15 cm × 4.6 mm)	0.1 wt% Ammonium acetate/methanol	0.1
HEF			1
BHEOX			10
HEA			0.1
HEPO			0.1
OZD			0.1
HEI			0.1
HEIA			1

Ion Chromatography (IC) was used for the quantification of the HSS anions and for MEA. The anions glycolate, propionate, formate, oxalate and acetate were analyzed on an ICS-5000 ThermoScientific System equipped with AS15 analytical column, an ASRS300 suppressor and a conductivity detector and a carbonate removal device. As mobile phase, the eluent generator with KOH cartridge connected to a Milliore ICW-3000 system was used. MEA analysis was conducted with a Thermo Scientific Dionex IonPac™ CS19 analytical column (2 x 250 mm) coupled with a Thermo Scientific Dionex IonPac™ guard column CG19 (2 x 50mm) and the CSRS 300 2mm suppressor. The mobile phase was 20 mM methanesulfonic acid and the cation chromatography method is described in Fytianos et al. [27].

The surface morphology and chemical composition of cylinders were examined by scanning electron microscopy (SEM) and energy dispersive spectrometry (EDS) in order to examine the effects of corrosion on surface morphology and chemical composition of the cylinders after 5 weeks experiment under stripper conditions. Small pieces were cut from the cylinders and cleaned with ethanol to remove any deposited corrosion products. Samples were placed on stubs and scanned without coating. Characterizations were carried out with a Hitachi S-3400N scanning electron microscope at an acceleration voltage of 20.0 kV and a working distance of 10.0 µm. EDS data were processed by using Aztec Energy Software.

Deposited corrosion products on the inner cylinder surfaces were collected gently by cotton swabs and crushed with a mortar and pestle for qualitative characterization via powder X-Ray Diffraction (XRD) (D8 Advance DaVinci, Bruker AXS GmBH). Analyses were conducted in the 2θ range of 20-80° using a Cu X-ray tube, with a step size of 0.013° and a step time of 0.78 s. The PDF-4+ database (from the International Centre for Diffraction Data) was used for the identification of species.

3. Results

In this section the MEA concentration changes and degradation products stability and formation are discussed. After that, IC results for the HSS are reported and ICP-MS for total metal concentration are presented. The results given in this chapter are the averages of the the two cylinder parallels. Finally, surface morphology and elemental mapping were evaluated by a combined use of SEM and EDS to examine the corrosion onto stainless steel.

As mentioned before the cylinders were weighed before and after the experiments as a leakage test. The average weight loss was less than 1 % based on the total cylinder weight, indicating that the cylinders were tight.

3.1 MEA concentration

The MEA concentration for all the samples after 5 weeks was between 14 to 15.5wt% and the MEA concentration decreased in the different solutions in a very similar way. When looking at the parallels we can see that the MEA loss differences where less than 1wt%. These results are in an agreement with results from the thermal degradation study of Fytianos et al. [16].

3.2 Degradation product formation and thermal stability

In table 3, the concentrations of the degradation products in mg/ L for the various solutions are shown after week 2 and 5 (the end of the experiment). For the mixtures of 30wt% MEA with 1wt% HEF and HEA only results from week 5 are given due to analytical error.

Table 3: LC-MS results in mg/L after week 2 and 5.

Solution	HeGly	HEF	BHEOX	HEA	HEPO	OZD	HEI	Bicine	HEIA	HEEDA
MEA										
Week 2	66	225	8	7	824	165	41		65408	14471
Week 5	15	817	8	11	238	80	29		128642	12430
MEA+HEEDA 1%										
Week 0										9130
Week 2	15	218	8	7	801	140	17		92968	15985
Week 5	6	774	8	11	282	67	12		133137	12016
MEA+OZD 1%										
Week 0						9130				
Week 2	36	261	8	7	457	158	19		99459	16380
Week 5	10	925	8	10	252	83	19		133769	11648
MEA+HeGly 1%										
Week 0	9130									
Week 2	4887	139	8	6	839	91	15		46681	15480
Week 5	663	838	8	10	920	96	14		125616	12547
MEA%+Bicine 1%										
Week 0								9130		
Week 2	72	241	8	7	820	142	16	7721	63811	15392
Week 5								5988	135626	12597
MEA+HEPO 1%										
Week 0					9130					
Week 2	86	277	8	13	10714	150	27		80142	16399
Week 5	25	862	8	13	8964	56	23		115221	12046
MEA+HEI 1%										
Week 0							9130			
Week 2	77	245	9	43	671	160	9097		67480	14255
Week 5	21	766	8	44	216	83	6832		104797	10453
MEA+HEIA 1%										
Week 0									9130	
Week 2	24	233	8	9	670	160	16		92932	14711
Week 5	8	717	8	11	258	84	11		136659	11756
MEA+BHEOX 1%										
Week 0			9130							
Week 2	56	1782	8	6	609	217	29		58972	14067
Week 5	18	2006	8	8	181	119	22		135695	14029
MEA+HEF 1%										
Week 0		9130								
Week 5	20	3072	8	10	176	105	23		135759	13607
MEA+HEA 1%										
Week 0				9130						
Week 5	15	705	8	5145	200	79	25		126884	11884

From Table 3, it can be observed that the dominant degradation products formed are HEIA and HEEDA in all experiments. This was expected, since the experiments were conducted at thermal degradation conditions. Furthermore, from the various solutions it can be seen that HEIA is a stable product and there is an increase from week 2 to week 5. Moreover, the MEA+OZD solution and MEA+HEEDA solutions have higher concentrations of HEIA compared to the other solutions. This is in good agreement with the work of Davis[17]. The thermal degradation reaction pathway of MEA includes the formation of OZD, then HEEDA and finally HEIA. OZD can be formed both from oxidative and thermal oxidation reactions. At 135 °C, OZD is not stable.

In addition to Table 3, HEHEAA was quantified for the MEA+HeGly solutions. In week 2, the concentration of HEHEAA was 755 mg/L and in week 5 HEHEAA the concentration was 73 mg/L. After week 5, the HEPO concentration increased only in the MEA+HeGly solution. It appears that MEA reacts with HeGly to form HEHEAA as a first step and then, in the second stage, HEPO forms from HEHEAA. The HEPO and HEHEAA concentrations are well correlated. HEHEAA was first identified at MEA based CO_2 capture facilities by Strazisar et al. [10] and the formation reaction was verified later experimentally by Vevelstad [28]. The reactions of HEHEAA and HEPO formation are presented in Figure 1.

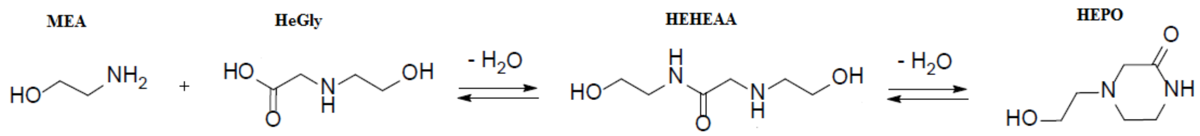

Figure 1: Formation reactions of HEHEAA and HEPO.

It is of great importance to know if a degradation product is thermally stable or if it reacts to form another product that might be corrosive. Originally 9130 mg/L (1wt%) of the various degradation products was added to the MEA solution. In the case of HEA it can be seen that final concentration of HEA after 5 weeks is high (5145 mg/L) compared to that in 30wt% MEA (11mg/L). This indicates that HEA is stable. HEI can be considered thermal stable also. Similarly, the final HeGly concentration in 30wt% MEA+ 1wt% HeGly is 660mg/L is more than 40 times higher than in 30wt% MEA (15mg/L). It should be noted that large amount of the added HeGly has decomposed after 5 weeks. When it comes to HEF we can see that it is more stable than HeGly, but less stable than bicine. BHEOX decomposes almost totally after 2 weeks. The typical oxidative degradation products HEA, HEI and HeGly are found in low concentrations.

3.3 IC for HSS anions

Formate formation is an indication of degradation, and can also be related to corrosion since it can form HSS with MEA. By examining quantitatively the formate concentration with IC, it can be observed that it increases each week. Most of the MEA+degradation product solutions showed similar formate concentration values as the 30wt% MEA solution. However, in the cases of BHEOX, HEF and HEA, significantly higher formate concentrations can be observed as shown in Figure 2.

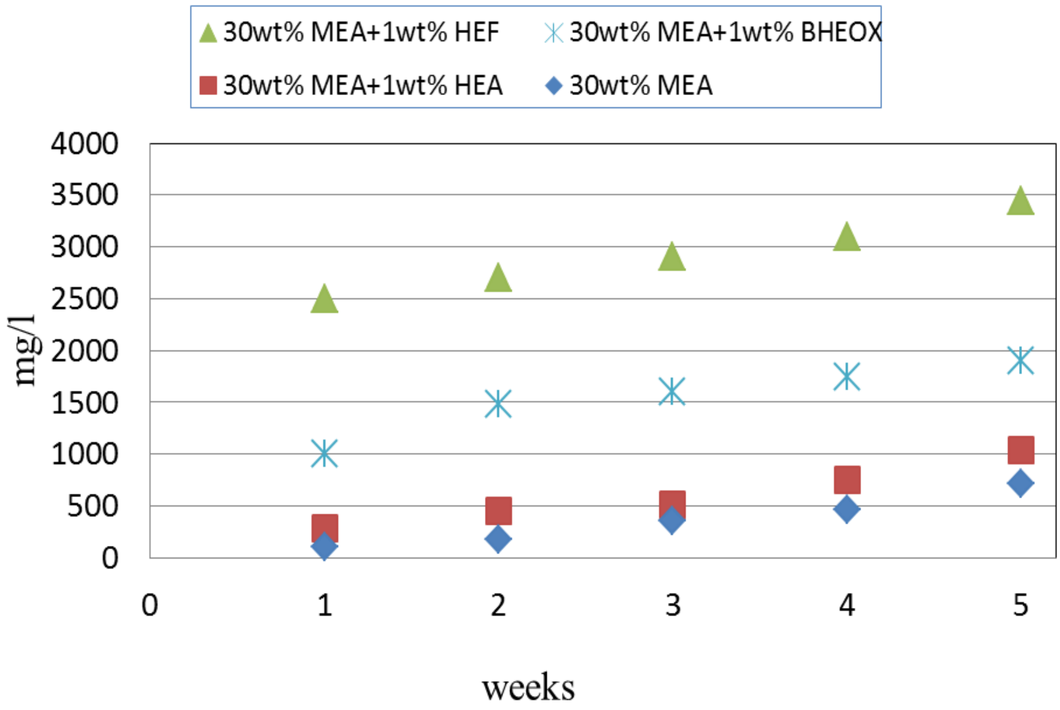

Figure 2: Concentration (mg/L) of formate for the different solutions.

HEF, BHEOX and HEA are formed from reactions with MEA with the corresponding carboxylic acid[4, 9]. Under oxidative degradation conditions, the HEF, BHEOX and HEA formations rates increase with higher oxygen concentration[13]. The HEF solution was expected to give the highest formate concentrations, since HEF is formed from the reaction between MEA and formic acid.

For BHEOX, anion IC results for the first week showed 306 mg/L oxalate which, under thermal decomposition, converted to formate in the second week. From Figure 2, it can be observed that the formate concentration for BHEOX solution from the first week to the second does not follow the trend from the remaining weeks. This is further evidence that thermal decomposition of oxalate forms formate. Higgins et al.[29] had shown that the decomposition of oxalate to formate is possible. For HEA, high acetate concentrations were measured, as expected.

3.4 ICP-MS for total metal concentration

Among the 4 metals (Fe, Cr, Ni and Mo) the dominant is iron followed by Ni and Cr. With ICP-MS, the individual metal concentrations were measured as an indication of corrosivity, see Figures 3-6. From the 10 degradation products that were tested, HEEDA, Bicine, HeGly and OZD solutions with MEA showed significantly higher metal concentrations than the 30wt% loaded MEA solution. Thus the Figures 3-6 show results only for MEA and for the previously mentioned solutions with the four specific degradation products. In Figure 3, results for total iron concentration are presented. It can be seen that after one week, the bicine solution has the highest total Fe concentration. Bicine solution continues to have higher Fe concentration in the following weeks, however in the second week, MEA+HeGly was the dominant corrosive solution. In week 5, MEA+bicine solution has the highest corrosivity. OZD, in the first and fourth week, has much higher iron concentration in comparison with MEA. Nevertheless, this is not the case for the rest of the weeks. There is an increasing tendency in iron concentration until the fourth week, and in the last week of the experiment there is a small decline. There is the possibility that some corrosion compounds are forming after 4 weeks and that is why in the last week smaller Fe concentration is observed for all the tested solutions. Although Fe is the dominant concentration, a significant increase of iron concentration with time is not observed. That can be explained because of a protective layer formation (it is discussed in chapter 3.6). Unlike iron concentration profile, total nickel concentration is increasing with time as it can be observed from Figure 4.

For Ni concentration of the various solutions, a major difference is shown in the first and fourth week. There, MEA+bicine solution followed by MEA+OZD appear to have significantly higher amounts of Ni compared to MEA solution. It is still unclear if by monitoring the metals Ni, Cr, and Mo, reliable results concering corrosion can be obtained.

In the case of Cr, as is presented in Figure 5, Bicine, HEEDA and HeGly seem to enhance solution corrosivity.From Figure 6, it can be seen that Mo concentration for MEA+bicine and MEA+OZD solutions is higher compared to MEA.

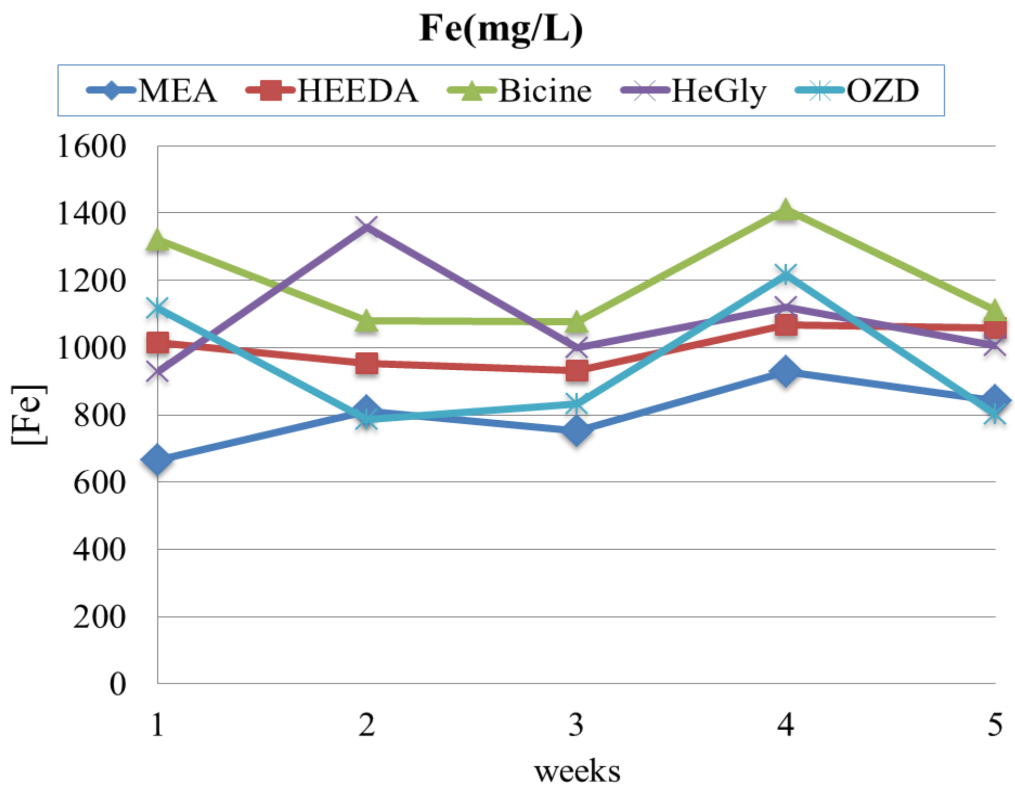

Figure 3: Total Fe concentration (mg/L) for the different solutions.

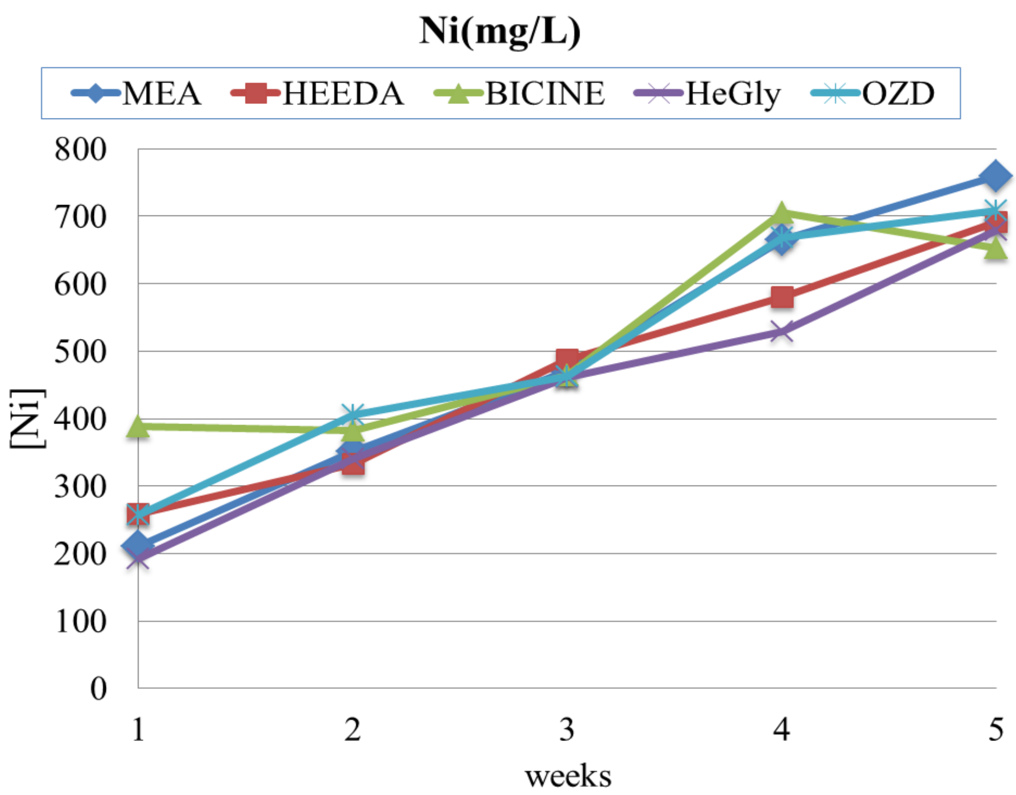

Figure 4: Total Ni concentration (mg/L) for the different solutions.

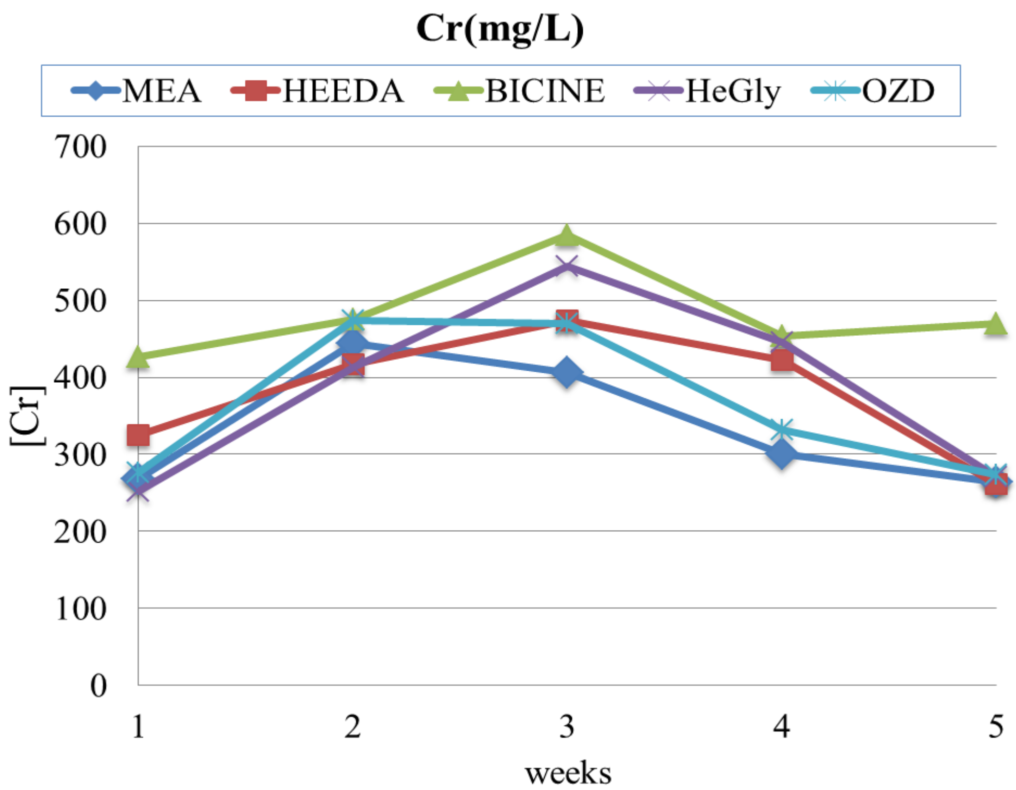

Figure 5: Total Cr concentration (mg/L) for the different solutions.

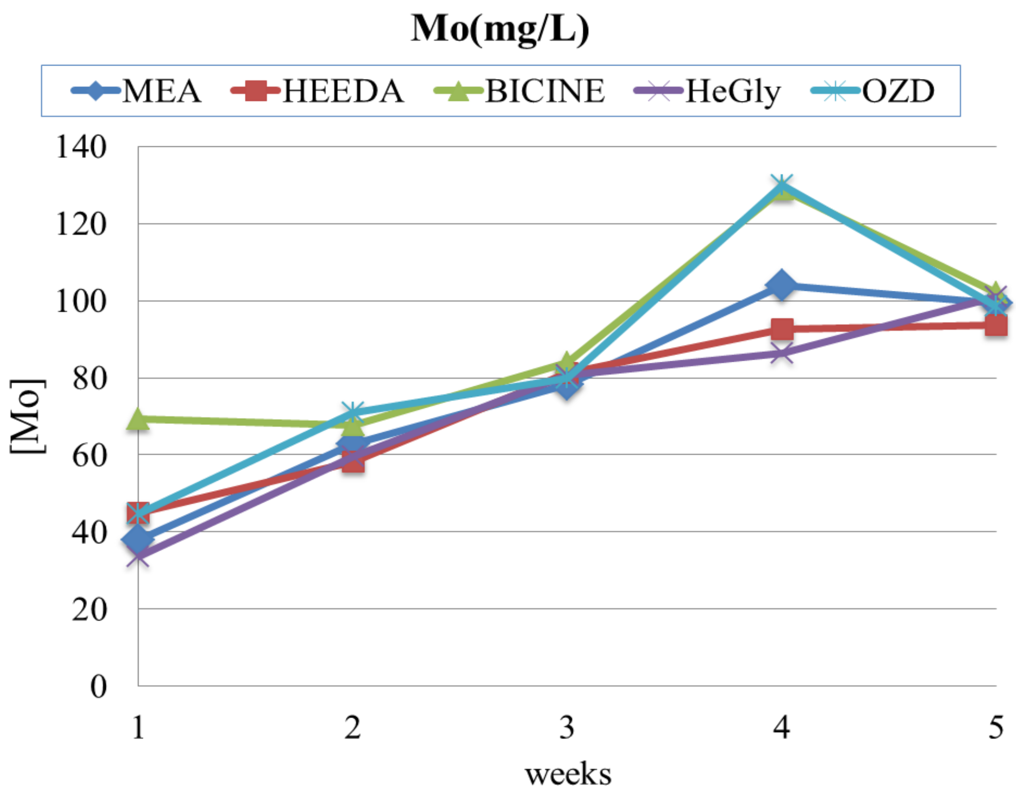

Figure 6: Total Mo concentration (mg/L) for the different solutions.

3.5 SEM-EDS

At the end of the experiment, surface morphology and elemental mapping were evaluated by a combined use of SEM and EDS, in order to examine the corrosive effects of the solutions on cylinder surfaces. Differences observed in the final surface morphology as a result of corrosion can be evaluated in terms of the varying extent of corrosion and corrosion mechanisms.

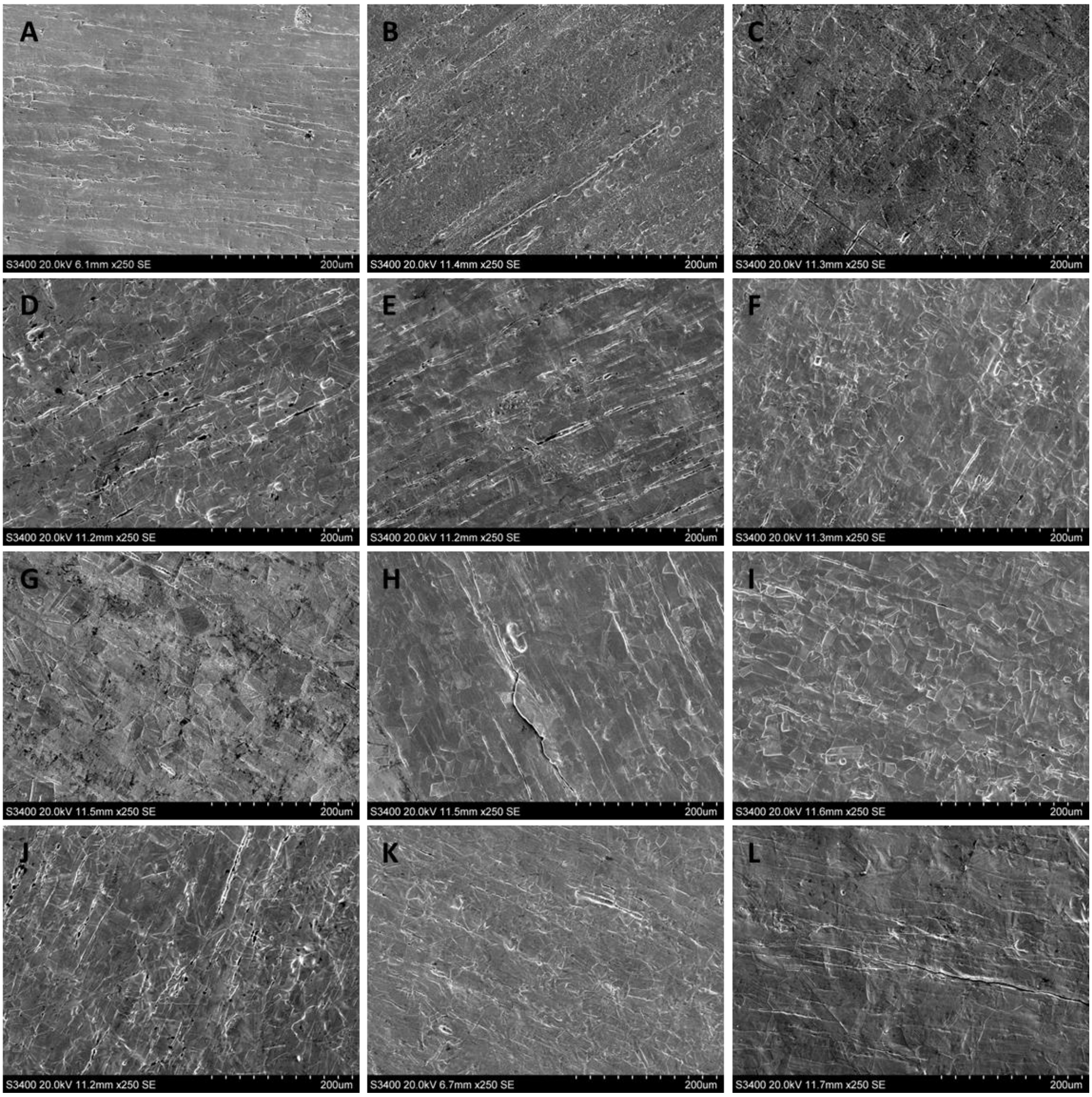

Figure 7: SEM images of cylinder surfaces (A) before immersion, and after 5 weeks of immersion in (B) 30 wt% MEA solution, (C) 30 wt% MEA with 1 wt% BHEOX, (D) 1 wt% HEA, (E) 1 wt% HEF, (F) 1 wt% HEGly, (G) 1 wt% HEI, (H) 1 wt% HEPO, (I) 1 wt% OZD, (J) 1 wt% HEIA, (K) 1 wt% HEEDA, and (L) 1 wt% Bicine.

When cylinders contained 30 wt% MEA solution, without addition of corrosion products, a rough surface was observed, which represents a uniform corrosion over the surface at the end of 5 weeks (Figure 7B). When secondary corrosion products were added to the solutions, crack formation and pitting were more prominent on cylinder surfaces. Both these features were most strongly revealed for the solutions containing 1 wt% HEA, HEI and HEIA (Figure 7 D, G, J). Significant crack formation was also observed in the presence of HEGly, HEPO, OZD and HEEDA in MEA solution (Figure 7 F, H, I, K).

SEM observations suggest that the presence of secondary corrosion products of MEA in solutions induced more localized corrosion on the cylinder surfaces which result in the emergence of crack formation and pitting. When it comes to the effect of HSS on corrosion, pitting corrosion was observed.[16] In addition, it was observed that pitting on the cylinder surfaces was always accompanied by corrosion cracks which suggests their promotion as a result of pit formation.

Cylinders immersed in MEA, MEA+HEA and MEA+OZD were compared in terms of elemental composition as representatives of different surface characteristics after corrosion, as shown in Table 4. From the table we can see that Elemental mapping by EDS revealed that the compositional homogeneity of the cylinder surfaces remained independent of the corrosion mechanisms and a single phase was detected for all samples.

Table 4. Elemental composition of 316 SS surfaces after 5 weeks of immersion in given solutions.

wt %	**MEA**	**MEA+HEA**	**MEA+ OZD**
Fe	58.9	59.8	60.6
Cr	16.8	16.7	17.0
Ni	11.3	11.5	11.9
Mo	2.1	2.1	2.3
C	5.9	5.1	3.9

3.6 XRD

Analyses of corrosion products that deposited on the surface of 316 SS tubes were carried out by powder XRD (Figure 8). Formation of highly crystalline siderite, $FeCO_3$, was observed on cylinder surfaces incubated in each solution. Cylinders which contained HEI, HeGly, BHEOX, Bicine, and HEPO also had weak signals of iron in diffraction data of the deposited products.

XRD analysis showed that the deposited product forming on the cylinder surfaces was siderite ($FeCO_3$). Siderite has been found to be the dominant product in CO_2-containing corrosion environments for carbon steel [30], but this may not be the case for stainless steel. The surface images in Fig. 7 do not show any solid formation but this is due to the sample preparation with removal of deposited corrosion products prior to SEM imaging. As an example, in Fig. 9 SEM images for the inner part of the cylinder for the case of MEA+HEF solution are shown. In this case the sample is not pre-treated with ethanol and a protective layer can be observed. The SEM image in Fig. 9B resembles siderite as presented in [31]. This layer was collected and analysis showed it to be $FeCO_3$. The formation of $FeCO_3$ in solution and deposition on the steel surface is probably due to the very nature of the thermal degradation experiment where the CO_2 pressure, and therefore liquid phase content, as well as the iron concentration, are high. Previous studies have shown that siderite acts as a protective layer and decreases the rate of corrosion on mild steel and carbon steel surfaces[32, 33]. Since $FeCO_3$ was identified on the corroded surfaces of all 316 SS samples, further research should be conducted on the effect of siderite in post-combustion CO_2 capture. Siderite can work as a protective layer and reduce the corrosion rate also in this case.

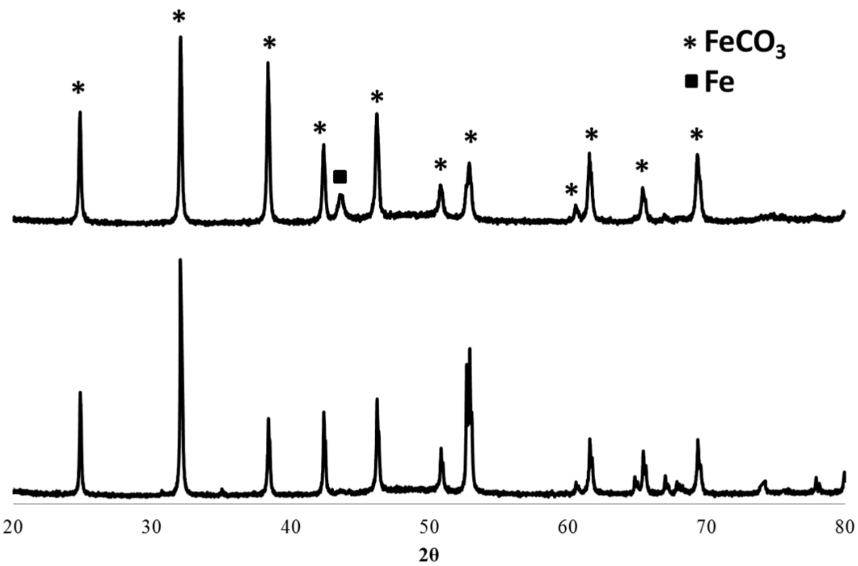

Figure 8: XRD spectra of corrosion products collected from cylinders immersed in 30 wt% MEA solution, and 30 wt% MEA with 1 wt% bicine from bottom to top, respectively. Asterisks denote peaks associated with $FeCO_3$ and square denotes crystalline Fe.

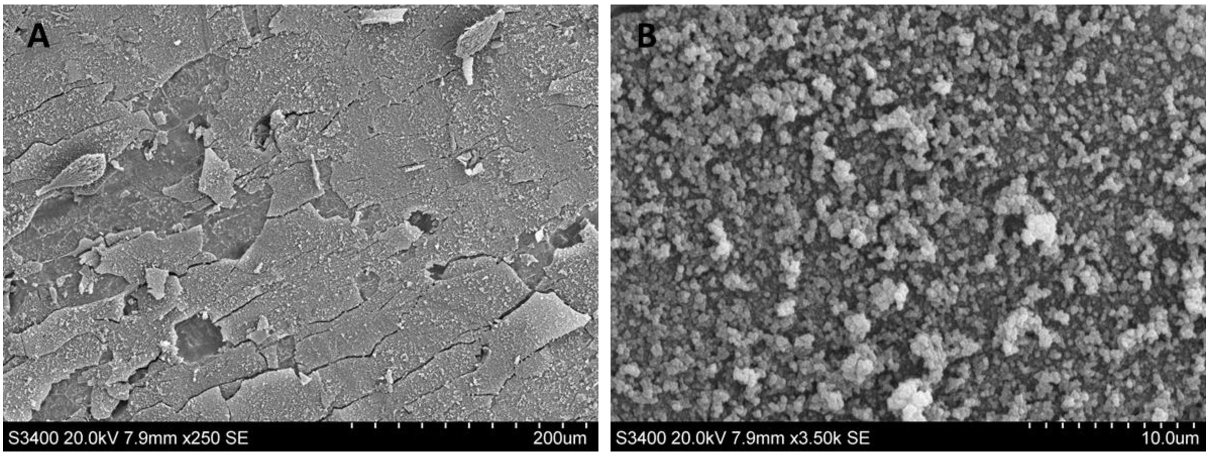

Fig. 9: SEM images of cylinder surfaces after 5 weeks of immersion in 30 wt% MEA solution with 1 wt% HEF at 250 times magnification (A) and 2000 times magnification (B).

4. Discussion

HeGly and HEPO are the dominant oxidative degradation compounds found in pilot plants[4]. HEPO, which is formed from the reaction of MEA and HeGly[4], although thermally stable, does not increase the corrosion rate according to ICP-MS results. Furthermore, HEIA, the dominant thermal degradation product, seems not to have a deteriorating effect on stainless steel. The imidazole HEI does not cause further corrosion when added to MEA solution. Bicine is a known corrosive product[34] in amine based gas treating plants. The findings of the current paper, showed that bicine plays a significant role in corrosion. From the ICP-MS results, it is shown that HEF and OZD can contribute to higher corrosion rates compared to the MEA solution without additives. HEEDA, which is a precursor for HEIA formation, is reported to cause corrosion problems in carbon steel[17]. ICP-MS results for Fe indicated that HEEDA increases the corrosivity of the solution. HEIA is the dominant thermal degradation compound in MEA based CO_2 capture plants, but it does not affect the solution's corrosivity.

Formate formation is directly correlated with degradation but it can also be associated with increasing corrosion. The addition of formic and oxalic acid (which decomposed to formic), had a higher impact on corrosion[16]. In the current work, HEF and HEA solutions, which had significantly higher formate concentration compared to only MEA, had also higher metal concentrations. However, formate concentration and total iron concentration cannot be correlated directly.

ICP-MS was the main technique used in this paper for measuring the corrosivity of the solutions. It is still unclear if by monitoring the metals Ni, Cr, and Mo, reliable results can be obtained. Since Fe is the dominant metal in stainless steel, either Fe itself or the sum of all the metals should be studied. Another important topic is the duration of the experiment. It might be that a two- instead of five-week experiment could yield similar results.

A summary of the degradation products that are tested for their corrosivity is given in Table 4. The results from the previous work [16] where the effect on corrosion for five acids that are found in CO_2 capture plants were studied, are also presented. In the previous work formic, oxalic, propionic, acetic and glycolic acid have been tested with similar experimental approach, like in the present paper. That fact that formic and oxalic acid proved to have a high effect on corrosion comes with good agreement with the findings of the current paper for the formamide HEF and the oxamide BHEOX.

SEM observations revealed that the presence of secondary corrosion products of MEA induce localized corrosion on the cylinder surfaces. It is known that the alloy composition and the concentration of specific corrosive species are highly effective on that type of corrosion. It was observed that when pit formation due to extreme localized corrosion occurred on the crystal surfaces, crack formation was also induced accordingly.

The main corrosion product formed on the cylinder surfaces was highly crystalline siderite, $FeCO_3$, regardless of the solution tested.

Table 4: Summary of MEA Degradation Product Corrosivity

Abbreviation	Compound	CAS	Stable at 135 °C	Corrosive
BHEOX	N,N′-Bis(2-hydroxyethyl)-oxamide	1871-89-2	No. Decomposes to oxalate and then to formate	It decomposes to corrosive compounds
HEA	N-(2-hydroxyethyl)-acetamide	142-26-7	Yes	Slightly
HEF	N-(2-hydroxyethyl)-formamide	693-06-1	Less than HEA	Slightly
HEGly	N-(2-hydroxyethyl)-glycine	5835-28-9	Very little	Yes
HEI	N-(2-hydroxyethyl)-imidazole	1615-14-1	Yes	No
HEPO	4-(2-hydroxyethyl)-2-piperazinone	23936-04-1	Yes	No, but forms HeGly
OZD	2-Oxazolidinone	497-25-6	No	Slightly
HEIA	N-(2-hydroxyethyl) imidazolidinone	3699-54-5	Yes	No
HEEDA	N-(2-hydroxyethyl) ethylenediamine	111-41-1	Degrades	Yes
Bicine	N,N-Bis(2-hydroxyethyl)glycine	150-25-4	Yes	Yes
Formic Acid [16]		64-18-6	Yes	Yes
Oxalic Acid [16]		144-62-7	No. Decomposes to formate	Yes
Propionic Acid [16]		79-09-4	Yes	No
Acetic Acid [16]		64-19-7	Yes	Slightly
Glycolic Acid [16]		79-14-1	Yes	No

5. Conclusions

The effect of MEA degradation products on corrosion has been studied. From the various products, HeGly, HEEDA, Bicine and BHEOX increased the corrosivity of 30wt% MEA solution. BHEOX, although not thermally stable, decomposes to oxalate and then to formate which form HSS. HEA and HEF enhance corrosion while HEIA, the major thermal degradation product, and HEI do not seem to aggravate corrosion. HEPO, although not corrosive itself, gives HeGly which is plays a major role on corrosion.

Acknowledgement

The work is done under the SOLVit SP4 project, performed under the strategic Norwegian research program CLIMIT. The authors acknowledge the partners in SOLVit, Aker Solutions, Gassnova, EnBW and the Research Council of Norway for their support.

References

1. Stéphenne, K., *Start-up of World's First Commercial Post-combustion Coal Fired CCS Project: Contribution of Shell Cansolv to SaskPower Boundary Dam ICCS Project.* Energy Procedia, 2014. **63**: p. 6106-6110.
2. Zhao, B., et al., *Study on corrosion in CO2 chemical absorption process using amine solution.* Energy Procedia, 2011. **4**(0): p. 93-100.
3. Desideri, U., *5 - Advanced absorption processes and technology for carbon dioxide (CO2) capture in power plants*, in *Developments and Innovation in Carbon Dioxide (Co2) Capture and Storage Technology*, M.M. Maroto-Valer, Editor. 2010, Woodhead Publishing. p. 155-182.
4. da Silva, E.F., et al., *Understanding 2-Ethanolamine Degradation in Postcombustion CO2 Capture.* Industrial & Engineering Chemistry Research, 2012. **51**(41): p. 13329-13338.
5. Kohl, A.L. and R.B. Nielsen, *Chapter 2 - Alkanolamines for Hydrogen Sulfide and Carbon Dioxide Removal*, in *Gas Purification (Fifth Edition)*, A.L. Kohl and R.B. Nielsen, Editors. 1997, Gulf Professional Publishing: Houston. p. 40-186.
6. DuPart, M.S., T.R. Bacon, and D.J. Edwards, *Understanding corrosion in alkanolamine gas treating plants: Part 1.* Journal Name: Hydrocarbon Processing; (United States); Journal Volume: 72:4, 1993: p. Medium: X; Size: Pages: 75-80.
7. DeHart, T.R.H., D. A.; Mariz, C. L.; McCullough, J. G, *Solving corrosion problems at the NEA Bellingham Massachussetts carbon dioxide recovery plant. .* NACE International Conference Corrosion '99 San Antonio, USA, , 1999(paper No 264).
8. Vevelstad, S.J., *Oxidative Degradation of MEA*, 2013.
9. Lepaumier, H., et al., *Comparison of MEA degradation in pilot-scale with lab-scale experiments.* Energy Procedia, 2011. **4**(0): p. 1652-1659.
10. Strazisar, B.R., R.R. Anderson, and C.M. White, *Degradation Pathways for Monoethanolamine in a CO2 Capture Facility.* Energy & Fuels, 2003. **17**(4): p. 1034-1039.
11. Sexton, A.J. and G.T. Rochelle, *Catalysts and inhibitors for oxidative degradation of monoethanolamine.* International Journal of Greenhouse Gas Control, 2009. **3**(6): p. 704-711.

12. Voice, A.K. and G.T. Rochelle, *Products and process variables in oxidation of monoethanolamine for CO2 capture.* International Journal of Greenhouse Gas Control, 2013. **12**(0): p. 472-477.
13. Vevelstad, S.J., et al., *Oxidative degradation of 2-ethanolamine: The effect of oxygen concentration and temperature on product formation.* International Journal of Greenhouse Gas Control, 2013. **18**(0): p. 88-100.
14. Rooney, P.C., M.S. DuPart, and T.R. Bacon, *Effect of heat stable salts on MDEA solution corrosivity.* Hydrocarbon Processing, 1997. **76**(4): p. 65-71.
15. Tanthapanichakoon, W., A. Veawab, and B. McGarvey, *Electrochemical Investigation on the Effect of Heat-stable Salts on Corrosion in CO2 Capture Plants Using Aqueous Solution of MEA.* Industrial & Engineering Chemistry Research, 2006. **45**(8): p. 2586-2593.
16. Fytianos, G., et al., *Effect of MEA's Degradation Products on Corrosion at CO2 Capture Plants.* Energy Procedia, 2014. **63**(0): p. 1869-1875.
17. Davis, J.D., *Thermal Degradation of Aqueous Amines used for Carbon Dioxide Capture. Ph.D. Dissertation The University of Texas at Austin.* 2009.
18. Zoannou, K.-S., D.J. Sapsford, and A.J. Griffiths, *Thermal degradation of monoethanolamine and its effect on CO2 capture capacity.* International Journal of Greenhouse Gas Control, 2013. **17**(0): p. 423-430.
19. Veawab, A., P. Tontiwachwuthikul, and A. Chakma, *Corrosion Behavior of Carbon Steel in the CO2 Absorption Process Using Aqueous Amine Solutions.* Industrial & Engineering Chemistry Research, 1999. **38**(10): p. 3917-3924.
20. Kladkaew, N., et al., *Corrosion Behavior of Carbon Steel in the Monoethanolamine−H2O−CO2−O2−SO2 System: Products, Reaction Pathways, and Kinetics.* Industrial & Engineering Chemistry Research, 2009. **48**(23): p. 10169-10179.
21. Saiwan, C., et al., *Part 3: Corrosion and prevention in post-combustion CO2 capture systems.* Carbon Management, 2011. **2**(6): p. 659-675.
22. Billingham, M.A., et al., *Corrosion and materials selection issues in carbon capture plants.* Energy Procedia, 2011. **4**(0): p. 2020-2027.
23. Kittel, J. and S. Gonzalez, *Corrosion in CO 2 Post-Combustion Capture with Alkanolamines – A Review.* Oil & Gas Science and Technology - Revue IFP Energies nouvelles, 2014. **69**(5): p. 915 - 929.
24. Fred Addington, D.E.H., P.E, *AGGRESSIVE CORROSION OF 316 STAINLESS STEEL.* NACE International Corrosion 2000 Paper No.00698, 2000.
25. Andreas Grimstvedt, E.F.d.S.a.K.A.H., *Thermal degradation of MEA, effect of temperature and CO2 loading.* TCCS7, SINTEF Materials and Chemistry, 7465 Trondheim, 2013.
26. Ma'mun, S., et al., *Selection of new absorbents for carbon dioxide capture.* Energy Conversion and Management, 2007. **48**(1): p. 251-258.
27. Fytianos, G., et al., *Quantitative determination of amines used in post-combustion CO2 capture process by ion chromatography.* International Journal of Greenhouse Gas Control, 2015. **42**: p. 372-378.
28. Vevelstad, S.J., et al., *Influence of experimental setup on amine degradation.* International Journal of Greenhouse Gas Control, 2014. **28**: p. 156-167.
29. Higgins, J., et al., *Theoretical Study of Thermal Decomposition Mechanism of Oxalic Acid.* The Journal of Physical Chemistry A, 1997. **101**(14): p. 2702-2708.
30. Gao, J., et al., *Corrosion behavior of carbon steel at typical positions of an amine-based CO 2 capture pilot plant.* Industrial and Engineering Chemistry Research, 2012. **51**(19): p. 6714-6721.
31. Berntsen, T., M. Seiersten, and T. Hemmingsen, *Effect of FeCO3 Supersaturation and Carbide Exposure on the CO2 Corrosion Rate of Carbon Steel.* Corrosion, 2013. **69**(6): p. 601-613.
32. Xiang, Y., et al., *Time-dependent electrochemical behavior of carbon steel in MEA-based CO2 capture process.* International Journal of Greenhouse Gas Control, 2014. **30**: p. 125-132.

33. Nešić, S. and K.-L.J. Lee, *A Mechanistic Model for Carbon Dioxide Corrosion of Mild Steel in the Presence of Protective Iron Carbonate Films—Part 3: Film Growth Model.* Corrosion, 2003. **59**(7): p. 616-628.
34. Bosen, S. and S.A. Bedell, *The Relevance of Bicine in Corrosion of Amine Gas Treating Plants*, NACE International.